UCRL-869 Rev.

UNCLASSIFIED

UNIVERSITY OF CALIFORNIA — BERKELEY

TWO-WEEK LOAN COPY

This is a Library Circulating Copy which may be borrowed for two weeks. For a personal retention copy, call Tech. Info. Division, Ext. 5545

RADIATION LABORATORY

DISCLAIMER

This document was prepared as an account of work sponsored by the United States Government. While this document is believed to contain correct information, neither the United States Government nor any agency thereof, nor the Regents of the University of California, nor any of their employees, makes any warranty, express or implied, or assumes any legal responsibility for the accuracy, completeness, or usefulness of any information, apparatus, product, or process disclosed, or represents that its use would not infringe privately owned rights. Reference herein to any specific commercial product, process, or service by its trade name, trademark, manufacturer, or otherwise, does not necessarily constitute or imply its endorsement, recommendation, or favoring by the United States Government or any agency thereof, or the Regents of the University of California. The views and opinions of authors expressed herein do not necessarily state or reflect those of the United States Government or any agency thereof or the Regents of the University of California.

UCRL-869 Rev.

UNIVERSITY OF CALIFORNIA
Radiation Laboratory

Contract No. W-7405-eng-48

90 MEV NEUTRON-PROTON SCATTERING AT LARGE PROTON ANGLES

Roger Wayne Wallace
(Thesis)

November 6, 1952

Berkeley, California

TABLE OF CONTENTS

	Page
I Introduction	3
II Apparatus and Procedure	4
III Recording of Data	7
IV Treatment of Data	9
V Conclusions	14
Table I	15
References	16
Figure Captions	17
Figures	20

90 MEV NEUTRON-PROTON SCATTERING AT LARGE PROTON ANGLES

Roger Wayne Wallace

November 6, 1952

I INTRODUCTION

Neutron-proton scattering cross sections have been measured using the 90 Mev neutrons from the 184-inch Berkeley cyclotron by several different investigators. Hadley, et al,[1] used two different arrangements of proportional counters. Their results are shown in Figure 8. It is seen that their points do not lie on a curve that is symmetrical about 90°. This experiment was performed to find out if the cross section does rise in the small angle region. It has been felt by some that the cross section curve (Figure 8) was flat to the left of 70° and did not rise. The results of this experiment serve to confirm the rising slope of the curve in the small angle range, in agreement with Hadley, et al. Brueckner, et al,[2] using a cloud chamber technique have observed an angular dependence of the n-p cross section similar to that observed by Hadley, et al. The results of the present experiment also agree well with the cloud chamber data.

II APPARATUS AND PROCEDURE

The main part of the apparatus consisted of a nuclear plate camera, similar in design to the camera used by Panofsky and Fillmore.[3] This camera and its associated collimator and shielding (Figure 1) were mounted on a support which was aligned under the 90 Mev neutron beam of the 184-inch cyclotron in order to allow the beam to pass along the axis of the collimator and camera. The collimator was similar to the paraffin collimator used by Brueckner et al.[2] The hole in the collimator was stopped down to a 1/2-inch diameter circle and additional lead bricks were added between the paraffin and the camera to reduce the background radiation. The internal arrangement of the camera (Figure 2) differed from that used by Panofsky and Fillmore[3] in that the plates were mounted farther from the beam radially and farther from each other. These dimensional changes were made in this experiment since the intensity of the neutron beam of the cyclotron is much less than the intensity of the proton beam of the linear accelerator used by Panofsky and Fillmore.[3] It was necessary in this cyclotron experiment to include more beam area with a consequent relaxation of the geometrical precision of the experiment.

At each end of the camera-scattering chamber there was a 0.005-inch duraluminum foil window. The cyclotron beam, collimated to 1/2-inch, passed into and out of the camera through these foils, without striking anything else in the camera except the scattering hydrogen gas. The exit foil was mounted on the end of a tube, as shown in Figure 2, in order to reduce the background tracks on the plates that might have come from particles scattered from the exit foil. Particles that might have been scattered from the entrance foil entered the plates at such an angle that tracks caused by them, when viewed under a microscope, were easily distinguished from those coming from the hydrogen gas contained in the scattering chamber, since the desired tracks and the foil scattered tracks entered the field of view from different angular directions. Thus the particles scattered from the entrance foil constitute a non confusable background.

Four point screw supports permitted the paraffin collimator and the camera to be aligned coaxially within 1/16-inch. The alignment was carried out with an optical telescope and was checked by exposing, during the first few minutes of the cyclotron run, an x-ray film located in a known position on the camera. A 1/16-inch alignment tolerance does not introduce a first order source of error since the plates were arranged symmetrically around the beam and the angular distribution data from all plates were combined. The plates were aligned in the camera by being held against a machined surface for which the geometric tolerance was less than 0.010-inch.

Two identical cameras were constructed, one for hydrogen exposures, the other for vacuum, background exposures. The exposures from which the data were taken were made for 405 minutes at an average of 27-1/2 R per hour, for the hydrogen run, and 65 minutes at an average of 28 R per hour, for the vacuum run. This made the hydrogen run 186 R and the neutron background run 30 R. The R is an arbitrary beam intensity unit approximately equal to 10^5 neutrons/cm^2 sec. The R is not used directly in this experiment other than to secure the ratio of the hydrogen to the vacuum exposure, which of course is independent of the magnitude of the R.

The first few trial runs with hydrogen in the camera resulted in completely blackened plates. At first it was thought that the blackening was caused by impurities in the hydrogen gas, so the hydrogen gas was passed through a hot palladium leak, thus separating all other elements with the possible exception of a minute trace of helium. Since the blackening still occurred to the same degree with this purified hydrogen it was concluded that the hydrogen itself must attack the emulsion. Webb[4] advised us later that it was possible that the photographic emulsions were fogged by pure hydrogen gas. The reason that Panofsky and Fillmore[3] did not experience this difficulty was that they used a lower hydrogen pressure than the two atmospheres used in this experiment, and somewhat shorter times during which the plates were exposed to the hydrogen. It was found that the blackening of the plates by the

hydrogen was temperature sensitive, and that a reduction of temperature to -15° to -20° C would allow the plates to be only slightly fogged after 8 hours exposure to the gas. Consequently a jacket, filled with a eutectic mixture of rock salt and ice, was installed around the camera intended for the hydrogen exposure.

III RECORDING OF DATA

The data (Table I, Column 2) were taken from the plates with a microscope operating at 570x and scanning a swath on the plates 140 microns wide. The recoil proton tracks were identified by their specific ionization, their point of entrance, dive angles into the emulsion, their azimuth angle in the microscope field, and their range. When a track seen to start in the field of the microscope had been recognized as that of a proton, by its ionization density, the microscope was focused up and down to check the fact that the track dived into the emulsion at an angle that was compatible with the geometric location of the photographic plate relative to the neutron beam. A typical relationship is shown in Figure 2. If the track passed this test, the plate was moved until the point at which the track entered the emulsion was centered under the microscope reticule cross hairs. The cross hairs were then rotated until one was tangent to the track as near to the point of entry as possible. Panofsky and Fillmore[3] explain how this may be done with a minimum of setting error. The azimuth angle of the entry point was then measured with a goniometer attached to one of the microscope eyepieces. This azimuth angle was the only datum recorded for each track.

The classical expression (Equation 1) for the energy E of a particle scattered by an equal mass particle gives the

$$E = E_o \cos^2 \theta \tag{1}$$

energy of a scattered proton as a function of the proton scattering angle θ, when the incident neutron energy is E_o. The incident neutron beam contains the distribution of energies given by Equation (2), which will be discussed later. The distribution

$$P(E_o) = K \exp\left\{-\left[(E_o - 90)/20\right]^2\right\} \tag{2}$$

of Equation 2, where $P(E_o)$ is the probability of an incident neutron having the energy E_o in Mev and K is a constant, causes the protons

that are scattered at any particular angle to also have an energy distribution. The energy distributions for proton recoil angles $\theta_L = 0^\circ$, 30°, and 45° in the laboratory system are shown in curves a, b, and c of Figure 3. Curves of this general form give the emulsion range distributions and also the grain density distributions to be expected of the protons scattered at various angles.

In taking the data, most of the tracks that were rejected were considered to be spurious on the basis of having the wrong ionization for their azimuth angle, or because they were too short for their azimuth angle. These rejection criteria did not need to be used on more than 2 percent of the otherwise acceptable tracks. Another reason for the rejection of tracks was that their dive angle into the emulsion was too steep for them to have been caused by protons coming from the beam cylinder (Figure 2). Tracks coming in the three other quadrants were easily eliminated, although their number was very limited. The scanning of the plates exposed in a vacuum indicated that the confusable background was less than 2 percent of the number of apparently acceptable tracks.

Two observers examined 2734 tracks. Of these, all 350 of the tracks observed in the 45° to 51° laboratory angle range, although thought to be proton recoils, were not included in the final results. These tracks were excluded since the specific ionization of tracks scattered at these angles, with energies of 35 to 50 Mev, is so low that an excessive number of tracks is missed by the observer. In addition all 157 tracks in the angular range of 79° to 85° in the laboratory system were not included in the final results since, as will be mentioned later, the correction factor for tracks that do not reach the plates due to scattering in the hydrogen gas is too large. The two observers read the same plate areas for 200 tracks and found that each missed about 5 percent of the tracks. The tracks missed were evenly distributed over all angles from 45° to 85° so this personal factor is a minor source of error in the angular distribution.

The plates used were Ilford, type C-2 with emulsions 50 microns thick. They were developed for 30 minutes at 68° F in developer consisting of one part of D19 mixed with six parts of water.

IV TREATMENT OF DATA

The uncorrected data are shown in Figure 4 curve d. The data are grouped into three degree intervals in the laboratory system, so any corrections in the angular measurement that are small compared to three degrees will not be noticeable. The relativistic correction (Figure 4, curve a) makes the observed laboratory scattering angle slightly smaller than the classical laboratory scattering angle.

The geometry of this experiment, although not nearly as precise as that of Panofsky and Fillmore,[3] did not make improtant corrections necessary. The tracks were observed in swaths 140 microns wide as the slides were moved under the microscope in a direction parallel to the x coordinate (Figure 2). The swaths were all located within 1/2-inch of the edges of the plates nearest the beam. The position of the particular swath, in which the microscope was working, within the 1/2-inch wide band on the plates was not recorded as part of the data. It must be pointed out that there was no attempt made to determine from which part of the 1/2-inch diameter beam cylinder each individual track came, nor was any record kept of the point on the plates at which each particle struck the plates. Thus there is a random rectangular distribution of the probability of a particle landing on a plate with a particular value of y. In addition the probability of a particle coming from a particular part of the cylindrical, uniform intensity beam is a sine distribution in z. These two distributions introduce a geometric uncertainty which must be included in a consideration of the precision of the results. The two probability distributions, one in y and one in z must be combined by a folding process, which is really a two step random walk effect. Due consideration must be given to the geometrical relation between the angle ϕ observed in the microscope and in the angle θ_L at which a particular proton is actually scattered from the beam. The mean difference between these two angles, shown by curve b in Figure 4, is seen to be less then $1/2^{\circ}$.

The upper limitation on the observable scattering angle θ is introduced by the limited range of the low energy, high angle,

protons in the hydrogen gas. The range-energy relations for protons in hydrogen at 2 atmospheres and -15° C and in nuclear emulsions are shown in Figure 5. It was decided, on the basis of the experience of Panofsky and Fillmore,[3] that emulsion tracks shorter than 30 microns should not be recorded. Tracks shorter than 30 microns are easy to miss in scanning the plates. When tracks shorter than 30 microns are found, it is difficult to make a good measurement of their emulsion entrance angle, and there are a large number of short background tracks against which it is tedious to discriminate if one tries to measure proton tracks shorter than 30 microns.

Since it was the purpose of this experiment to extend the cross section curve to smaller angles it is important to investigate the limitations on the acceptability of the data in the small neutron angular range. There are four effects to be considered in deciding how far into the small angle region the data can be considered dependable.

1. At about $\theta_L = 80°$ the energy of the scattered protons becomes so small that all of them do not have a range in the hydrogen gas long enough to allow them to strike the plates.
2. Also due to their low energy they experience appreciable amounts of small angle scattering in the hydrogen gas.
3. Small angle scattering in the photographic emulsion also becomes important. These two types of scattering introduce errors in the measurements of the scattering angles.
4. Furthermore, in the region of 80°, as a result of the reduced proton energies, as mentioned above, the ranges of the particles in the emulsions are in many cases too short to allow for accurate identification and measurement.

The combined result of these four effects must be ascertained in order to evaluate the data properly.

The neutron beam produced by the bombardment of a 1/2-inch beryllium target with 180 Mev deuterons is known to have a broad energy distribution. This distribution has been calculated by Serber,[5] and measured by Hadley, et al.[1] For energies above the maximum

of the distribution curve the calculated and measured results agree, but the measured results are higher than the theoretical ones for energies below the maximum. For the purposes of this experiment it was assumed that the probability of an incident neutron having a particular energy has the form of Equation 2. This relation (Figure 3, curve e), approximates the high energy distributions of both Serber[5] and Hadley, et al,[1] but only the measured values of Hadley, et al, for energies less than 90 Mev. It was further assumed that the neutron-proton scattering cross section is inversely proportional to the energy in the energy range considered. Thus the neutron distribution that is effective in producing recoil protons is given by:

$$P'(E_o) = K\,(1/E)\,\exp\left\{-\left[(E_o - 90)/20\right]^2\right\} \qquad (3)$$

(Figure 3, curve a). The integral of this curve gives the fraction of the recoil protons coming from that part of the beam for which the energy is below any given value, (Figure 3, curve d). This relation will be used to calculate the fraction of the protons with energies too low to reach the plates at large scattering angles where the stopping power of the hydrogen is high. From the range-energy relations for protons, in hydrogen and emulsion (Figure 5) the energy of the protons entering the emulsion coming from different energy regions of the beam can be calculated as a function of the laboratory proton scattering angle, θ_L. From these energies the ranges in the emulsion for the protons from different beam energy intervals can be plotted as a function of the angle (Figure 6, curves a). Since no tracks shorter than 30 microns are to be considered, there will be a correction factor by which the track counts at various angles ϕ must be multiplied. The cutoff is shown crossing the three beam fraction curves. From the cutoff curve the initial correction curve is calculated (Figure 6, curve b). This correction does not include the effects of gas and emulsion scattering.

The combined probability distributions due to the small angle gas and emulsion scattering are shown in Figure 7, curves a. These are for particles that left the scattering centers at $\phi_L = 78^\circ$ and 79°. The probability distributions are multiplied point by point by the correction curve (Figure 6, b) and plotted on top of curves 7a, resulting in the peaks to the right of the maxima of the symmetric curves. The areas of these new curves as a function of the original scattering angle ϕ (Figure 7, curve b) are then the final correction factors. In reality the correction factor has a very small influence on the final cross section curve. The data that go into the single point for neutrons at 26° in the center of mass system are 71, 57, and 46 tracks at proton angles, $\theta_L = 76^\circ$, 77° and 78° respectively. When the correction factor is applied the data are changed to 71, 62, and 62 respectively. This application of the cutoff correction factor raises the point at the neutron center of mass angle of 26° by 11 percent.

The corrected track counts, grouped in three degree intervals, as a function of proton laboratory angle (Table I, column 4) were converted to numbers proportional to the n-p cross section as a function of the neutron center of mass angle by the relation derived from the geometry of Figure 2:

$$(d\sigma/d\omega)_{cm} \propto N(\phi)_{\Delta\theta} \left[(z^2 + y^2)/z\right] (1/\Delta (\cos \theta_{cm})) \quad (4)$$

In Equation 4, $N(\phi)_{\Delta\theta}$ is the data divided by true scattering angles θ instead of observed angles ϕ. Actually the difference between these angles (Figure 4, curve b) is such a slowly varying function of the angle that the correction for it was not applied. The geometrical factor $(z^2 + y^2)/z$ is independent of the scattering angle. As a result of the geometrical parameters, when the two 1/2-inch geometrical tolerances are combined properly, they produce a probable error of 1.54 inches in the geometrical factor, $(z^2 + y^2)/z$, whose mean value is 13.12 inches. This probable error only introduces a very small error into the relative cross section data which is combined with the statistical error and properly normalized

is listed in Table I, column 7. The values of the $\Delta(\cos\theta)_{cm}$ factor of Equation 3 for the transformation from laboratory to center of mass angles are shown in Table I, column 5 and $1/\Delta(\cos\theta)_{cm}$ is plotted in Figure 4, curve e. The corrected data divided by these factors and multiplied by 1.192×10^{-3} to normalize the results to the absolute cross sections of Hadley, et al,[1] are given in Table I, column 6, and plotted with their probable errors in Figure 8, in combination with the points measured by Hadley, et al.

V CONCLUSIONS

The n-p scattering cross section can be measured by the nuclear emulsion method for 90 Mev neutrons between neutron angles in the center of mass system from approximately 26° to 80°. In general the results agree with those secured by Hadley, et al,[1] with counters. The slopes of the curves agree between 36° and 60°. The results of this experiment confirm the increasing slope of the cross section curve in the small angle region; however the asymmetry of the curve about 90° is based on the Hadley data since the curve from this experiment is normalized to the Hadley results.

The author wishes to express his appreciation to Keith Brueckner who aided in the design of the apparatus, to Jack Steller who helped with the runs and the microscope reading, and to Professor W. K. H. Panofsky, under whose direction the work was carried out. This thesis is based on work performed under the auspices of the Atomic Energy Commission.

TABLE I

1	2	3	4	5	6	7
Proton Laboratory Angle Range	No. of Tracks Observed	Mean Neutron C.M. Angle	No. of Tracks Corrected	$\Delta(\cos\theta)_{cm}$ Transformation Factor	$\frac{d\sigma^*}{d\omega}$ in cm $10^{-27}cm^2$	Combined Probable Error
46-48	114	86	114	0.06963		
49-51	181	80	181	0.06874		
52-54	241	74	241	0.06710	4.28	0.19
55-57	260	68	260	0.06472	4.80	0.20
58-60	280	62	280	0.06163	5.42	0.22
61-63	266	56	266	0.05787	5.48	0.22
64-66	270	50	270	0.05347	6.02	0.24
67-69	248	44	248	0.04848	6.11	0.26
70-72	240	38	240	0.04298	6.77	0.29
73-75	248	32	248	0.03699	8.01	0.34
76-78	174	26	195	0.03060	7.60	0.39
79-81	120	20				
82-84	32	14				

Total 2734 Tracks Observed

* Normalized to the cross sections of Hadley, et al,[1] by the factor 1.192×10^{-3}.

REFERENCES

1. J. Hadley, E. L. Kelly, C. E. Leith, E. Segrè, C. Wiegand, and H. York, Experiments on N-P Scattering with 90 and 40 Mev Neutrons, Phys. Rev. 75, 351 (1949)
2. K. Brueckner, W. Hartsough, E. Hayward and W. Powell, Neutron-Proton Scattering at 90 Mev, Phys. Rev. 75, 555 (1949)
3. W. K. H. Panofsky and F. L. Fillmore, The Scattering of Protons by Protons near 30 Mev, Phys. Rev. 79, 57 (1950)
4. Julian Webb, Eastman Kodak Company, private communication
5. R. Serber, The Production of High Energy Neutrons by Stripping Phys. Rev. 72, 1007 (1947)

FIGURE CAPTIONS

Figure 1 Arrangement of the paraffine collimator and lead bricks in front of the scattering camera. The alternate cameras are shown. The vacuum camera is shown in the bombardment position. The jacketed hydrogen camera is shown at one side. The wood supports for the apparatus are not shown. Twelve nuclear track plates were arranged symmetrically around the beam at 30° intervals, of which one is indicated in the figure.

Figure 2 Geometrical location of the nuclear track plates relative to the neutron beam. The variables used in the measurements and calculations are shown. All variables are in the laboratory system. The relations between the scattering angle θ and the observed angle ϕ are indicated.

Figure 3 Functions dependent on the energy. Curves (a), (b), and (c) are the probability of a recoil proton being scattered at 0°, 30°, or 45° having a particular energy. It is seen that the absolute dispersion in energy decreases as the scattering angle increases. Curve (d) gives the percentage of the protons scattered at 0° with energy above a definite value of E. This curve is secured directly from curve (e), the energy distribution of the "90 Mev" neutron beam from the 184-inch Berkeley cyclotron.

Figure 4 Functions depending on the laboratory angle at which the protons recoil. Curve (a) gives the difference between the classical recoil angle and the relativistic recoil angle. This correction is seen to be small. Curve (b) shows the mean correction made necessary by the geometry. Curve (c) gives the mean path distance through the hydrogen gas in the scattering chamber from the points of impact in the cylindrical beam region to the photographic plates. Curve (d) is a histogram of the raw data grouped in three-degree intervals. The data from 46° to 52° and from 79° to 82° was considered unreliable

for reasons mentioned in the text. The data from 76° to 79° was corrected for limited proton range in the hydrogen and for small angle scattering in the gas and emulsion, as shown. Curve (e) is the multiplication factor for converting the laboratory coordinate data of curve (d) to the center of mass data of Figure 8. The conversion factor is calculated for the same three-degree intervals into which the data is divided.

Figure 5 Range-energy curves for protons in hydrogen gas at 2 atmospheres and -15° C and in nuclear track emulsion.

Figure 6 The experimental cutoff of tracks at the large proton angle limit is based on the three curves (a) of proton range in the emulsion for protons scattered at angles shown, coming from the three positions on the beam energy distribution shown on curve (d), Figure 3. The 30-micron cutoff shown above is explained in the text. Curve (b), the multiplicative correction factor that must be applied to the data as a result of the cutoff, is secured from the three curves (a) directly, and includes no correction for gas scattering.

Figure 7 The symmetrical parts of curves (a) are the superposition of the small angle gas and emulsion scattering probabilities for protons scattered at 78° and 79° in the laboratory system. Since some of these particles are viewed on the plates at angles greater than 79° and are thus partially not counted as a result of the cutoff shown on Figure 6, a correction must be applied to the recorded data. The correction curve shown in Figure 6(b) has been multiplied by curves 7(a) point by point and the results are the asymmetrical bumps shown on the right side of each curve. The areas of the resulting curves are the correction factors that must be applied to the recorded data and these factors are given by curve (b).

Figure 8 The final corrected data are shown by the circles above. The results of Hadley, et al,[1] are shown by the triangles. It is seen that the slopes of the results of the two experiments agree between 36° and 60°.

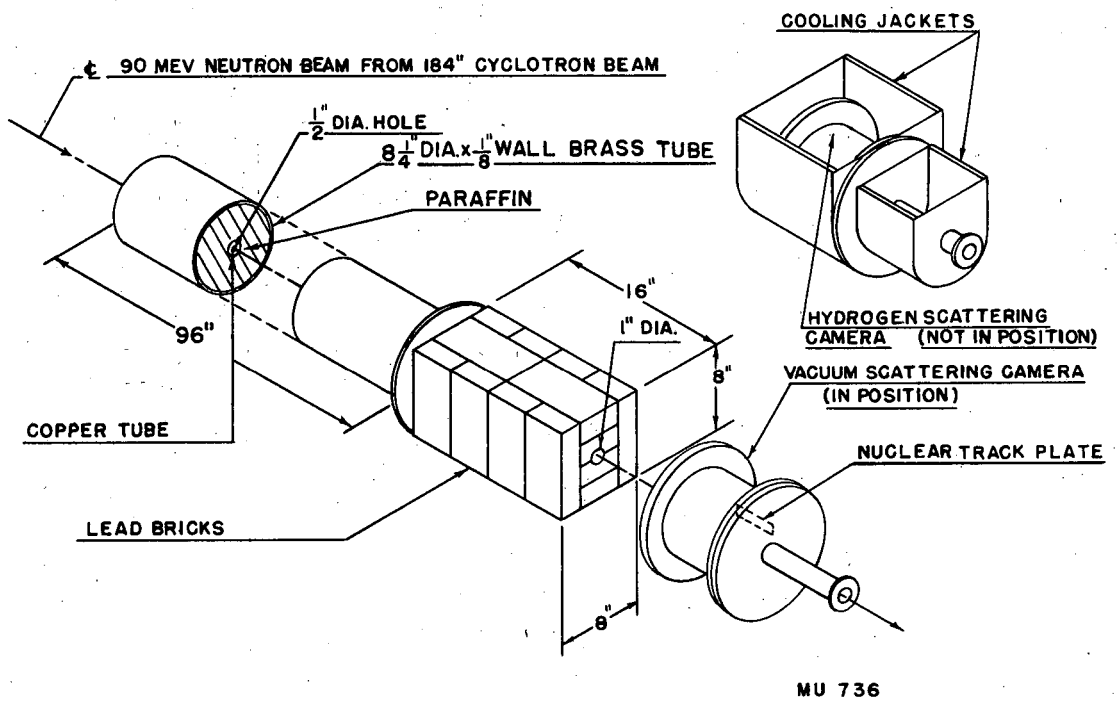
COOLING JACKETS
℄ 90 MEV NEUTRON BEAM FROM 184" CYCLOTRON BEAM
1/2" DIA. HOLE
8 1/4" DIA. x 1/8" WALL BRASS TUBE
PARAFFIN
16"
1" DIA.
96"
8"
HYDROGEN SCATTERING CAMERA (NOT IN POSITION)
VACUUM SCATTERING CAMERA (IN POSITION)
COPPER TUBE
NUCLEAR TRACK PLATE
LEAD BRICKS
8"
MU 736

FIGURE 1

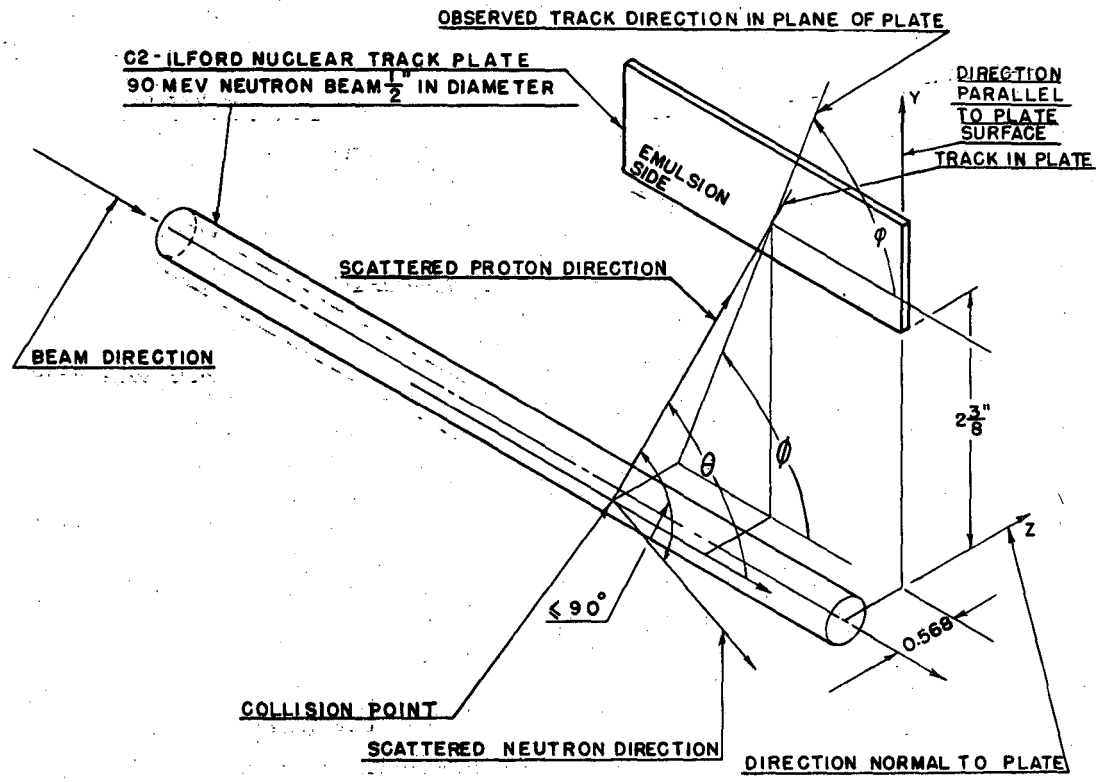

MU 737

FIGURE 2

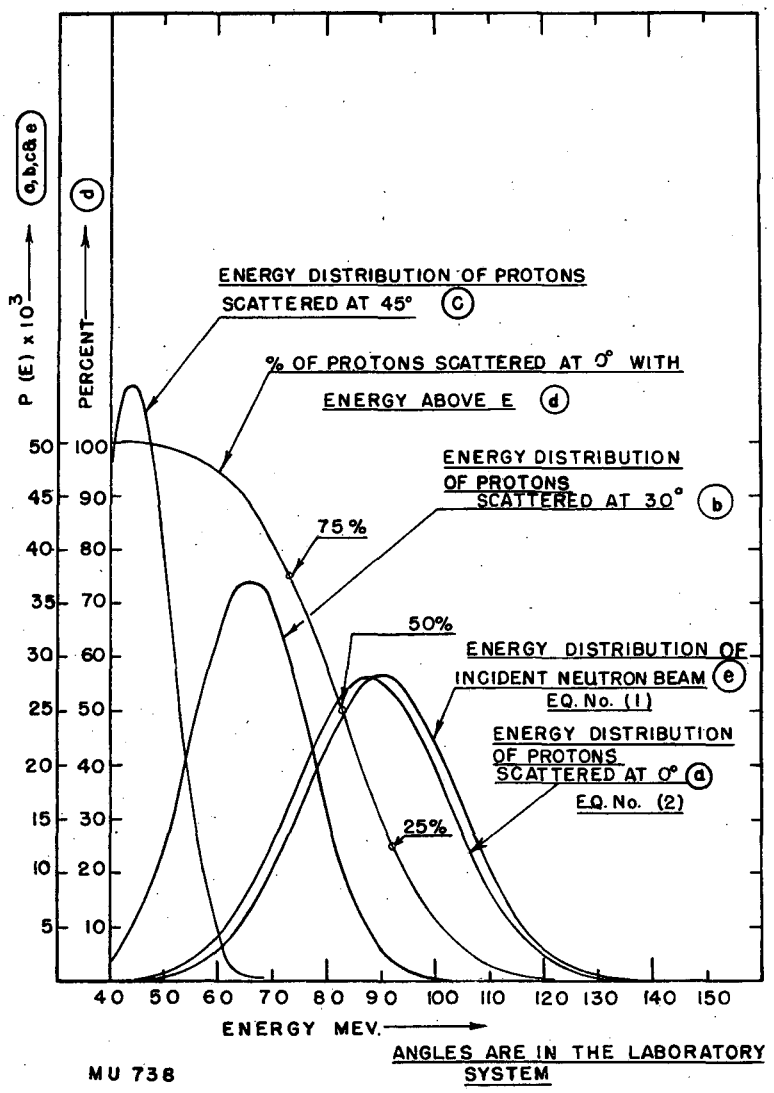
P (E) x 10^3 → a,b,c & e
PERCENT → d
ENERGY DISTRIBUTION OF PROTONS SCATTERED AT 45° c
% OF PROTONS SCATTERED AT 0° WITH ENERGY ABOVE E d
ENERGY DISTRIBUTION OF PROTONS SCATTERED AT 30° b
75%
50%
25%
ENERGY DISTRIBUTION OF INCIDENT NEUTRON BEAM e
EQ. No. (1)
ENERGY DISTRIBUTION OF PROTONS SCATTERED AT 0° a
EQ. No. (2)
50 45 40 35 30 25 20 15 10 5
100 90 80 70 60 50 40 30 20 10
40 50 60 70 80 90 100 110 120 130 140 150
ENERGY MEV.
ANGLES ARE IN THE LABORATORY SYSTEM
MU 738

FIGURE 3

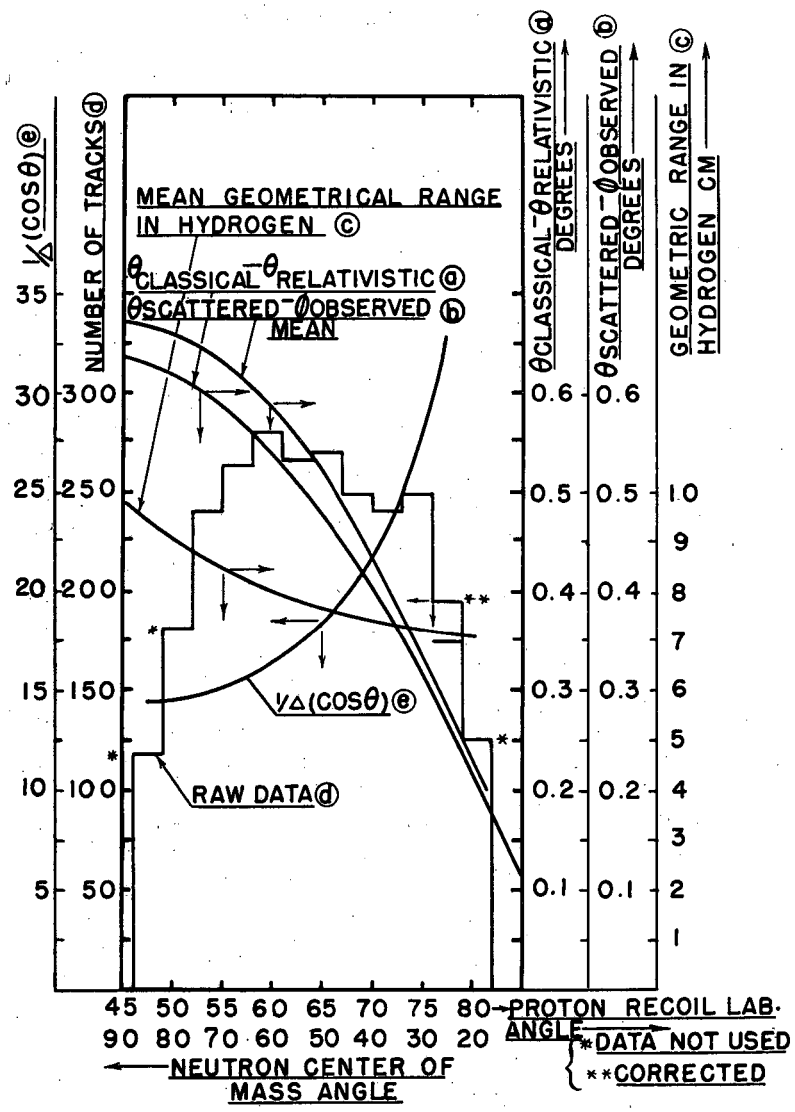
MEAN GEOMETRICAL RANGE IN HYDROGEN ⓒ
θCLASSICAL-θRELATIVISTIC ⓐ
θSCATTERED-ØOBSERVED ⓑ
MEAN
1/Δ(COSθ) ⓔ
RAW DATA ⓓ
NUMBER OF TRACKS ⓓ
1/Δ(COSθ) ⓔ
θCLASSICAL-θRELATIVISTIC ⓐ DEGREES
θSCATTERED-ØOBSERVED ⓑ DEGREES
GEOMETRIC RANGE IN ⓒ HYDROGEN CM
35 30 25 20 15 10 5
300 250 200 150 100 50
0.6 0.5 0.4 0.3 0.2 0.1
0.6 0.5 0.4 0.3 0.2 0.1
10 9 8 7 6 5 4 3 2 1
45 50 55 60 65 70 75 80 → PROTON RECOIL LAB. ANGLE
90 80 70 60 50 40 30 20
← NEUTRON CENTER OF MASS ANGLE
* DATA NOT USED
** CORRECTED

MU 740

FIG. 4

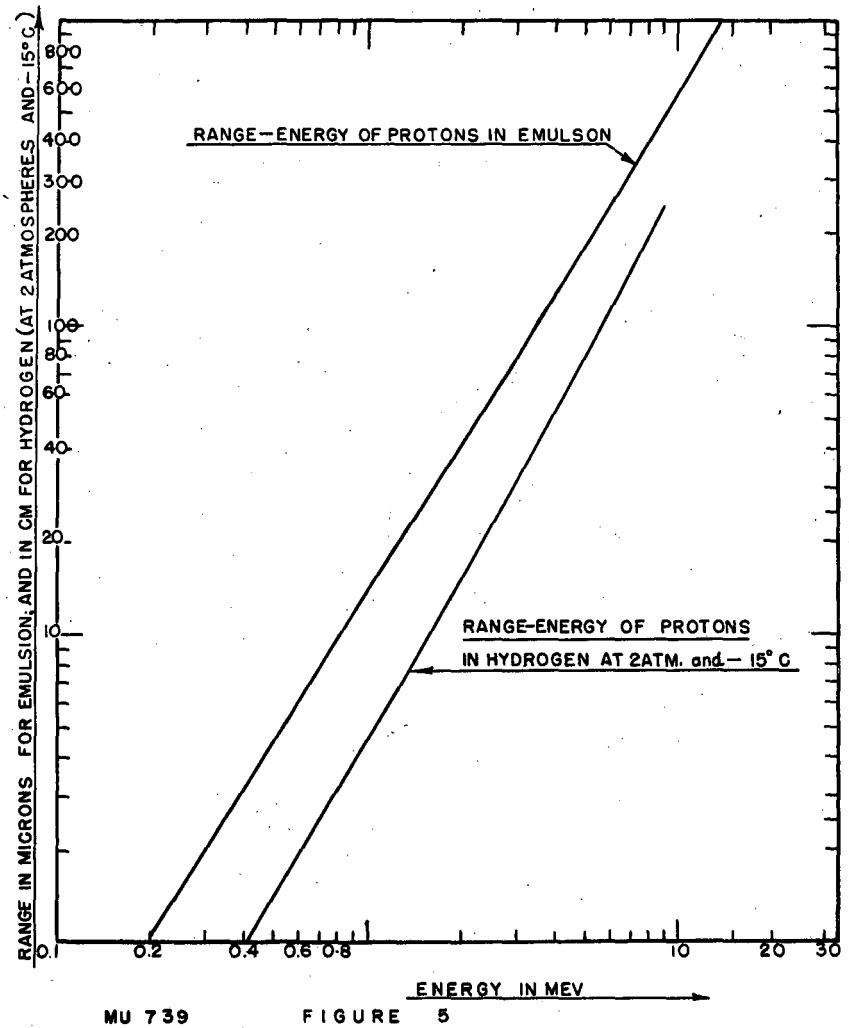

MU 739 FIGURE 5

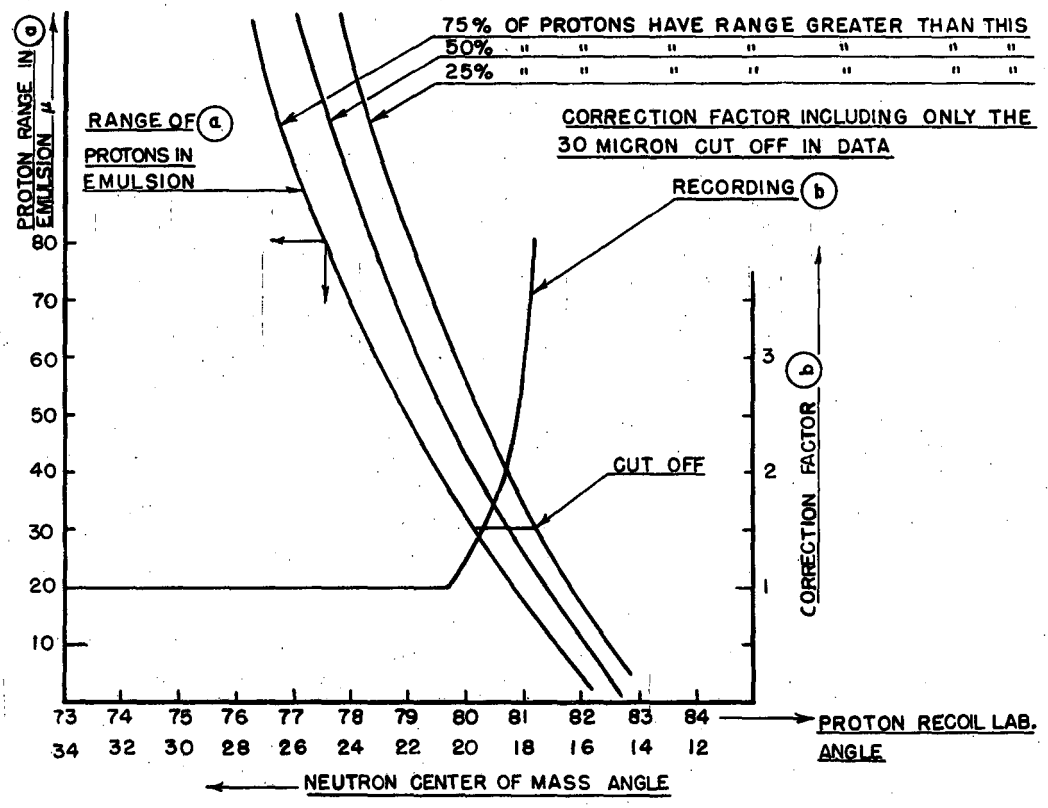

FIGURE 6

MU 741

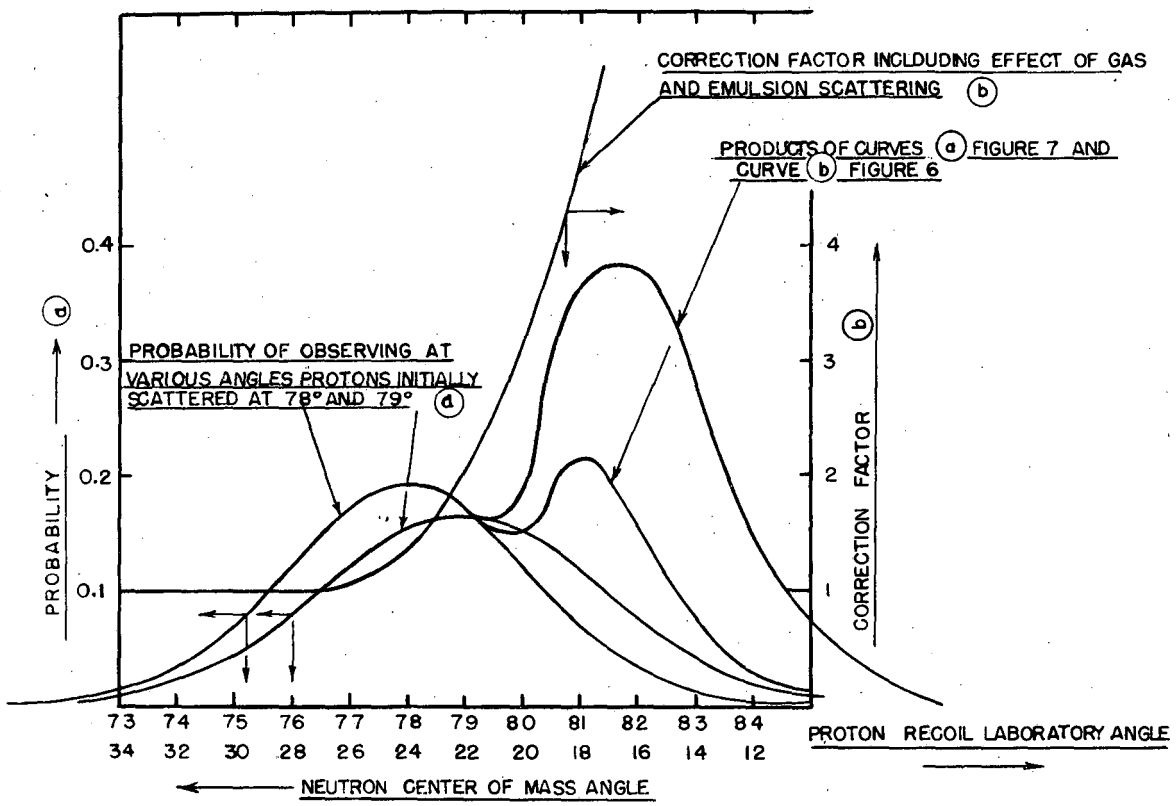

MU 742

FIGURE 7

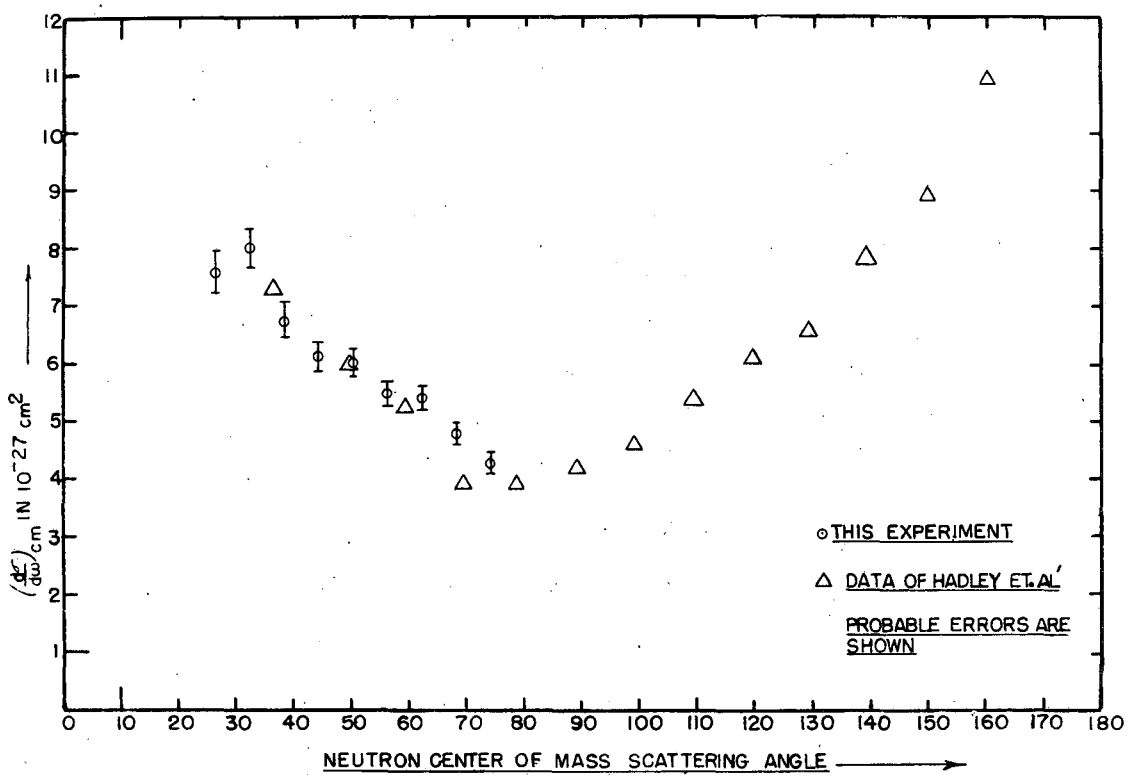

MU 743

FIGURE 8

165211